Original Article – Laboratory Science

Assessment of Corneal Biomechanical Properties with Inflation Test Using Optical Coherence Tomography

Yanping Huang PhD,[1¶] Like Wang,[1¶] Lei Tian MD, [2¶] Yifei Huang PhD,[3] and Yongping Zheng PhD[1*]

[1]Interdisciplinary Division of Biomedical Engineering, Hong Kong Polytechnic University, Kowloon, Hong Kong, China.

[2]Beijing Institute of Ophthalmology, Beijing Tongren Eye Center, Beijing Tongren Hospital, Capital Medical University; Beijing Ophthalmology & Visual Sciences Key Laboratory; National Engineering Research Center for Ophthalmology, Beijing 100730, China

[3]Department of Ophthalmology, Chinese PLA General Hospital, Beijing, 100853, China

¶Yanping Huang, Like Wang and Lei Tian contributed equally to this work.

[*]Corresponding author: Prof. Yongping Zheng

Interdisciplinary Division of Biomedical Engineering,

Faculty of Engineering,

Hong Kong Polytechnic University, Hong Kong

E-mail: yongping.zheng@polyu.edu.hk

Tel: +852 27667664

Running title: Biomechanical Assessment of Cornea

Conflict of interest: No

Funding sources: National Natural Science Foundation of China (No. 81271052), Hong Kong Polytechnic University Joint PhD Supervision Scheme (G-UB58), the Hong Kong Scholars Program (No. XJ2012044), the China Postdoctoral Science Foundation funded project (No. 2012T50212), the Priming

Scientific Research Foundation for the Junior Researcher in Beijing Tongren Hospital, Capital Medical University (2015-YJJ-ZZL-008) and Beijing Key Laboratory of Ophthalmology and Visual Science (2016YKSJ02).

Abstract

Background: Biomechanical properties are essential for the cornea to maintain its normal shape and function and they play an important role in a number of corneal diseases and treatment schemes. There is still a need to develop better methods for the measurement of corneal mechanical properties.

Methods: We propose to introduce the optical coherence tomography (OCT) in inflation test for the measurement of corneal biomechanical properties. Preliminary experiment was conducted to demonstrate the feasibility of the proposed experimental approach**.** Ten cornea-mimicking silicone phantoms with different stiffness and five fresh porcine corneas were tested. Intro-ocular pressure was changed from 10 to 90 mmHg using two different loading rates to observe the pressure-apex displacement relationship and calculate the stiffness of the corneas.

Results: The stiffness of corneal phantoms obtained by the inflation test ranged from 0.2 to 1 MPa which was highly consistent with the results from the mechanical tensile test ($y = 0.70x$, $p < 0.001$). Porcine corneas showed highly viscoelastic behavior with obvious hysteresis in inflation. An apparent stiffness of 0.63 ± 0.07 MPa and 1.05 ± 0.08 MPa was obtained for the porcine cornea with loading rates of 3.3 and 33 mmHg/min, respectively. Mapping of corneal surface displacement was also generated for both the phantom and porcine corneas.

Conclusions: The preliminary study showed that it is feasible to incorporate the high resolution OCT imaging in inflation test to measure the corneal stiffness, with a future potential to locally measure the biomechanical properties of the cornea.

Keywords: Biomechanical properties; Cornea; Inflation; Optical coherence tomography; Phantom

INTRODUCTION

Cornea is a transparent tissue located on the outmost side of an eyeball which provides the function of protection for internal ocular tissues and power of optical refraction for clear vision. The biomechanical properties of the cornea, especially its stiffness, are important in maintaining the shape and then the normal vision of the eye by resistance to intraocular pressure (IOP).[1] Corneal diseases such as keratoconus and treatment outcomes of refractive surgeries such as LASIK are well known to be closely associated with the biomechanical properties of the cornea.[2,3] A better understanding of the corneal biomechanical properties becomes of great importance for clinical applications.[4] A number of methods have been developed recently for the measurement of corneal biomechanical properties in vivo;[5] however, most of these methods provide biomechanical behavior indices of the cornea rather than intrinsic material properties such as the Young's modulus. Therefore, an accurate and reliable measurement method to obtain the intrinsic biomechanical properties, even *in vitro* or *in situ*, is still much demanded for basic research as well as providing good references for validating new measurement techniques in vivo.

Traditionally the most straightforward method to study the corneal biomechanics is a uniaxial extension test of a thin corneal strip *in vitro* based on its stress-strain relationship.[6] However, the cornea may lose its structural integrity when cut into a small strip since the collagen fibrils within the stroma have been broken, which may cause some changes of the material properties compared to its original status. Compared to the extension method, an inflation test measures the biomechanical properties through expanding the entire cornea by IOP change, while keeping the integrity of the tissue.[7] Similarly, the IOP-displacement relationship of the cornea is obtained from the inflation experiment to calculate corneal

biomechanical parameters. Inflation test has been successfully applied to detect the increase of corneal stiffness after collagen cross-linking.[8,9] The inflation test has also been used to demonstrate human corneal behavior is affected by age and loading rate.[10] However, traditional inflation tests generally adopt some simple method such as a laser beam to quantify the change of the corneal shape at its apex,[11] which lacks the ability to monitor the different expansions of the cornea at different locations. There are also other studies which used commercial device such as Pentacam to capture the cross-section of the cornea in inflation experiment.[12] However, this Scheimpflug imaging technique is severely affected by geometrical and optical distortions which make complex correction necessary for the extraction of quantitative information from this measurement.[13-15]

Optical coherence tomography (OCT) has been widely used for ophthalmologic imaging of both anterior and posterior segments of the eye in clinic.[16,17] This technique could provide non-contact, high-resolution, real time imaging of the corneal structure, such as thickness. 2D, 3D or en-face OCT imaging of the cornea can be used for the diagnosis of the corneal pathologies such as keratoconus and assessment of treatment outcome such as refractive surgery.[18] Furthermore, OCT has also been applied to soft tissue biomechanics detection when combined with an external air puff as the mechanical stimulation method.[19-21] This method has been used to measure corneal biomechanical properties and characterize the change of corneal stiffness before and after cross-linking.[22] Besides, shear wave elastography was introduced to measure corneal elasticity based on phase-sensitive OCT.[23]

The purpose of this study is to propose and validate a new method which adopts OCT imaging in inflation test to investigate the corneal biomechanical behavior both globally and locally. This paper is arranged as follows. Firstly, the proposed experimental setup,

samples, experimental tests and data processing to calculate corneal biomechanical parameters are described. Then results are presented and compared with reference measurement or under different testing conditions. After that, thorough discussion about the methods, results and limitations of this study is given before the final conclusions are given at the end.

METHODS

OCT system and experimental setup

A custom-made spectral domain (SD) OCT system with a superluminescent diode (Part no. IPSDS804C, Inphenix Inc., Livermore, CA, USA), which had a central wavelength of 840 nm, a bandwidth of 45 nm and an output power of 4.5 mW, was used for corneal cross-section imaging working at an A-scan rate of 24 kHz. The axial and lateral resolution of the OCT system was 8 μm and 21 μm, respectively. Real time B-mode images were acquired with a scan size of 600 × 1024 pixels (width × depth) corresponding to 8 mm × 3.3 mm in each image. Figure 1 shows a schematic of the proposed experimental setup. The corneal sample was sealed on its rim on the outer side of an artificial anterior chamber (K20-2125, Katena products Inc., Denville, NJ, USA). Within the seal it was filled with normal saline solution, simulating the aqueous humor in the anterior chamber of human eye exerting an IOP on the cornea. A motor driven pumping system was designed to control IOP by adjusting the height of the saline solution. The IOP was quantified by a pressure sensor (MPX5100, Freescale semiconductor Inc., Austin, TX, USA) installed on the sidewall of the water tube (Figure 1) and sampled with a data acquisition card (USB-6211, National Instruments, Austin, TX, USA) in a personal computer. The personal computer was also

utilized to operate the OCT system and control the pumping system with custom-designed program developed by Labview (Version 2009, National Instruments, Austin, TX, USA).

Sample preparation and inflation test

The proposed method was tested using both cornea-mimicking silicone phantoms and porcine corneas in vitro. The advantage of using silicone phantoms is that the stiffness can be easily controlled independently so as to validate the proposed method in a broad range of corneal stiffness. Based on the normal geometry of the cornea, the corneal phantom was designed with a central thickness of 500 μm and a peripheral thickness of 1000 μm. The curvature radius of the anterior surface was 8 mm and that of the aspherical posterior surface varied from 6 mm to 7 mm, consequently. The diameter of the cornea was 12 mm and the height of the unloaded anterior segment was 3.8 mm (Figure 2).[24] The corneal phantom was fabricated by the mixture of a type of silicone (RTV-2 M4600 A, Wacker Chemicals Hong Kong Ltd., Hong Kong) and oil (AK-35, Wacker Chemicals Hong Kong Ltd., Hong Kong) using different ratios in order to control different stiffness. After mixture, the material was casted into a mold designed with the abovementioned geographical parameters and cured at 60 °C for 1 hour.[24,25] Corresponding silicone strips with a width × length × thickness of 5 mm × 35 mm × 3 mm were also made at the same time using the same mixture, therefore having the same stiffness with the corneal phantoms (Figure 2). These silicone strips were tested under extension using a standard mechanical testing machine (Alliance RT/5, MTS Corp., Eden Prairie, MN, USA) and the measured stiffness is compared to that obtained by the inflation method to validate the proposed method. For

system validation, a total of 10 pairs of corneal phantoms and silicone strips were successfully fabricated and tested.

Five fresh porcine eyes were collected from a local slaughterhouse and maintained in 0.7% normal saline at 4 ºC before testing. The specimens were tested in no more than 2 hours after sacrifice to reduce the swelling of cornea. Cornea was cut from the porcine eyeball along the corneal limbus with ~2 mm sclera remained for fixation. They were moisturized by an ultrasonic humidifier in room temperature during the whole inflation test.

Before test, the probe of the OCT system was adjusted to image the central area of the cornea passing its apex. The imaging depth of 3.3 mm was enough to observe the whole corneal surface movement during the inflation test. IOP was then changed from 10 mmHg to 90 mmHg to inflate and deflate the cornea in one typical test. To simulate the conditions of quasi-static and dynamic loading, two different loading rates of 3.3 and 33 mmHg/min for IOP change were used to test the cornea.[10] Data of OCT images and IOP were sampled synchronously at the rate of 1 Hz and saved for off-line data processing. In another test, a 3D scan of the corneal volume (8 mm × 8 mm × 3.3 mm) was also collected in a quasi-static loading condition at the specific IOP of 10 and 90 mmHg, respectively, in order to obtain the 2D mapping of the corneal surface displacement at different locations. For the corneal strip, it was pre-stressed by clamping the sample with a slight force of 20 mN with an initial length of 30 mm and then extended by 1 mm at a rate of 0.5 mm/min. The tensile stiffness was calculated based on the slope of the simple stress/strain curve within a strain range of <3%.[24]

Data processing method

OCT images were processed by a series of signal processing methods to identify the corneal surface (Figure 3). The raw image (Figure 3a) was pre-treated by enhancing the image brightness and then applying median and Wiener filter to reduce speckle noises (Figure 3b). Then the phase symmetry method was adopted to sharpen the boundaries (Figure 3c).[26] Finally, the boundary of the anterior surface was detected as the longest smooth line (Figure 3d).

The position of the corneal anterior surface detected in the vertical direction (in pixel) was denoted as *L(m, t)*, where *m* and *t* represent the lateral position in the image (in pixel) and the time, respectively. The displacement of the corneal anterior surface $D(m,t)$ at time point *t* is determined by:

$$D(m,t) = L(m,t) - L(m,0) \quad (1)$$

where $t = 0$ means the starting point at an IOP of 10 mmHg used as a baseline. A typical corneal displacement is shown in Figure 4, which clearly shows the expansion of the corneal anterior surface within an inflation test.

Based on a previous study, the cornea inflation test can be described by a thin shell theory and Hooke's law as shown in Figure 5.[27] When the condition of corneal thickness *T* and radius of its curvature R meets $T/R < 0.1$, the relationship of IOP-apex displacement can be approximated using the following equation:

$$D = \frac{pR^2}{2ET}(1-\nu) \quad (2)$$

where D is the apex rise, p the IOP, E the Young's modulus, and ν the Poisson's ratio of cornea. ν = 0.49 was used assuming cornea as an almost incompressible material in this study. Correspondingly, the Young's modulus of the cornea could be calculated based on the IOP-apex displacement relationship and the corneal shape in an inflation test. For the corneal phantoms, a thickness of 0.5 mm and a curvature of 8 mm were used for calculation. For porcine corneas, these two parameters were measured based on real OCT images. Corneal average thickness was measured as the distance between the two interfaces along the axis passing through the apex and the corneal curvature was calculated by a regressed circle passing through the corneal anterior surface.

A 2D mapping of the corneal anterior surface displacement at two different IOPs of 10 mmHg and 90 mmHg under a quasi-static loading condition was performed by the following calculation:

$$D_{2D}(x,y) = L_{IOP=90}(x,y) - L_{IOP=10}(x,y) \quad (3)$$

where x and y indicate the position of the corneal anterior surface in a projected plane which is perpendicular with the optical axis passing through its apex. This analysis of corneal displacement mapping might provide valuable information on the local distribution of corneal changes under the applied IOP.

RESULTS

A typical curve representing the relationship of IOP and apex displacement of a corneal phantom is shown in Figure 6a. All the corneal phantoms showed consistent, nearly purely elastic response under the currently tested IOP range. It was also found there was no

significant difference of IOP-apex displacement relationship under the two IOP loading rates. The Young's modulus of corneal phantoms obtained from the inflation test varied from 0.2 to 1 MPa, which showed a very high consistency ($y = 0.70x$, $R^2 = 0.98$, $p < 0.001$, Pearson correlation, Figure 7) with that from the extension test. This result indicated that the current inflation test method was a valid method to measure the mechanical properties of the intact cornea.

For the porcine corneas, obvious nonlinear IOP-apex displacement relationship was observed (Figure 6b), which was significantly different from that of the silicone corneal phantoms. The part of loading and unloading was also separated, indicating an obvious phenomenon called hysteresis. Furthermore, this relationship was also affected by the inflation rate (Figure 6b). An apparent Young's modulus was calculated in the loading phase in this situation. It was 1.05 ± 0.08 MPa and 0.63 ± 0.07 MPa corresponding to the inflation rate of 33 and 3.3 mmHg/min, respectively.

Typical results of mapping of corneal anterior surface displacement under the two different IOPs of 10 mmHg and 90 mmHg for the corneal phantom and the porcine cornea were shown in Figures 8 and 9, respectively. The overall 3D corneal shape before and after IOP change is also shown. As expected, the corneal displacement at those points with various distances from the corneal center was different. A bigger value of displacement was observed at the center of the corneal surface compared with its surroundings, indicating local variation of corneal surface displacement in the inflation test.

DISCUSSION

In this study, optical coherence tomography was introduced as the imaging modality in an inflation test to investigate the corneal biomechanical properties. With a simplified inflation analysis model,[27] corneal stiffness could be measured from the IOP-apex displacement relationship and the corneal structural parameters. The corneal phantom test showed a high consistence of the corneal Young's modulus measured using inflation with that obtained from the uniaxial extension test. Further experiment on the 2D mapping of the corneal surface displacement showed it could measure the local response of the cornea in the inflation test, thus having the potential to measure the local change of its biomechanical properties, which warrants further investigation.

In the inflation test, the corneal structural change was imaged by an integrated OCT system instead of being measured at a single point at the corneal apex. OCT is a non-invasive, fast and high resolution imaging technique which has been broadly used in tissue cross-section imaging especially in ophthalmology. The resolution of the proposed OCT system was 8 μm in the longitudinal direction which could obtain the change of corneal structure in details in the inflation test. Therefore, it was advantageous to incorporate this imaging modality in the traditional inflation test to have a detailed study of the tissue response at different locations of the cornea.

The range of IOP change was set to be from 10 to 90 mmHg under which the cornea was reported to be stable for its mechanical behavior.[27,28] Boschetti et al. reported that the whole pressure-apex displacement curves in an inflation test could be divided into two linear regions with the cut-off point at 10 mmHg.[28] The mechanical response of cornea was

dominated by extracellular matrix below IOP of 10 mmHg and by collagen fibrils after that. Therefore, the start value of IOP = 10 mmHg was used in this study because normal IOP is larger than 10 mmHg and collagen fibrils were the focus of our interest. Two different pressure loading rates (3.3 mmHg/min and 33 mmHg/min) were used with each representing a static and a dynamic loading, respectively, during an inflation experiment to characterize the corneal behavior difference.[29] For the results from corneal phantoms, the results showed that the measured stiffness did not change with that of the loading rate, and the curves of loading and unloading parts were nearly the same with each other, which might be due to the elastic material used in fabricating the corneal phantom.[30] The corneal stiffness from the inflation test was significantly correlated with that from traditional mechanical test ($y = 0.70x$, $R^2 = 0.98$), which showed that the measured elastic stiffness from the inflation test could be used as an effective parameter to indicate the elasticity of the tested material. However, it was significantly smaller than that from the extension test, which might be due to the non-ideal analysis using the thin shell theory in inflation test causing some deviation in the calculation of the elastic modulus in Equation (2). Fortunately, based on the correlation analysis, it seems that this kind of deviation can be corrected by a simple compensation of the linear coefficient when applying the Equation (2) for the extraction of Young's modulus in an inflation test.

For porcine eye specimen, the corneal behavior demonstrated a phenomenon of loading rate dependence and hysteresis in the inflation test as shown in Figure 6b, which were commonly seen in the biomechanical test of biological tissues. Boyce et al.[31] also reported that the viscoelastic behavior of bovine corneas in the form of loading rate-dependent

hysteresis. A significantly larger value of elastic modulus was observed with a faster loading rate than the slower loading rate, which was expected. In this case, the liquid in the tissue could not be repelled from the loaded region in a quick loading so it would exert an extra resistant force in response to the loading, increasing the measured corneal stiffness. In the present study, there was approximately 58% energy loss during a cycle of loading and unloading at the loading rate of 3.3 mmHg/min, while only 16% energy loss was observed at the loading rate of 33 mmHg/min. The observed viscoelastic parameters could be used to characterize the change of biomechanical properties in various diseases or treatment assessment. For example, Kling et al.[8] used similar parameters of Young's modulus and hysteresis to study the effect of UV collagen cross-linking on change of corneal biomechanical properties. They found that the Young's modulus of cornea became higher after cross-linking and hysteresis in cross-linked eyes was lower than that in non-treated eyes.

2D Surface displacement mapping was obtained in the present study to quantify the localized mechanical response of the cornea during inflation test as shown in Figures 8 and 9. It was found that the area surrounding the corneal apex had larger surface displacement compared to the peripheral area. This result was natural because of the corneal structure and its boundary condition. Normally, cornea is thin at the central area and thick at the edge.[32] Although the curvature around the corneal center was the same, the peripheral area of cornea was relatively flattered when compared with the central area. Besides, the corneal specimen was fixed on an artificial anterior chamber with the edge fixed in the current test. The complex corneal structure including its varied thickness and curvature would

contribute to the different displacement observed at different locations.[27] Another observation was that compared to the corneal phantom, the mapping of displacement distribution in the porcine cornea had more regional variations, which might be due to the lower quality image signals for real porcine samples and/or the larger inhomogeneity of the distribution of mechanical properties in different regions of the porcine cornea. Considering the anisotropic and complex biomechanics of the cornea, further study might be needed in combination with other investigation tools such as finite element analysis to obtain the different biomechanical properties at different locations of the cornea, which is the advantage to introduce this high resolution imaging method, i.e. OCT, into the inflation test as proposed in the current study.

In summary, an improved method of adopting OCT imaging in inflation test was proposed in the current study to better investigate the corneal mechanical behavior. The proposed method was validated by phantom studies in comparison with a uniaxial extension test. Preliminary data were also presented to show the complicated nonlinear viscoelastic behavior when porcine corneas were tested under different IOPs and different loading rate. This method might assist in building better numerical mechanical modeling to provide more precise assessment of local corneal biomechanical properties and predictions for corneal surgery to avoid unnecessary side effect. In future studies, corneal numerical modeling can be established to accurately interpret or simulate corneal biomechanics on basis of the surface displacement distribution obtained in the current method.

ACKNOWLEDGEMENTS

This study was partly supported by grants from the National Natural Science Foundation of China (No. 81271052), Hong Kong Polytechnic University Joint PhD Supervision Scheme (G-UB58), the Hong Kong Scholars Program (No. XJ2012044), the China Postdoctoral Science Foundation funded project (No. 2012T50212), the Priming Scientific Research Foundation for the Junior Researcher in Beijing Tongren Hospital, Capital Medical University (2015-YJJ-ZZL-008) and Beijing Key Laboratory of Ophthalmology and Visual Science (2016YKSJ02). The authors would like to thank Ms. Sally Ding for editing the manuscript.

REFERENCES

1. Dupps WJ, Wilson SE. Biomechanics and wound healing in the cornea. *Exp Eye Res* 2006; **83**: 709-20.
2. Deenadayalu C, Mobasher B, Rajan SD, Hall GW. Refractive change induced by the LASIK flap in a biomechanical finite element model. *J Refract Surg* 2006; **22**: 286-92.
3. Andreassen TT, Simonsen AH, Oxlund H. Biomechanical properties of keratoconus and normal corneas. *Exp Eye Res* 1980; **31**: 435-41.
4. Kotecha A. What biomechanical properties of the cornea are relevant for the clinician? *Surv Ophthalmol* 2007; **52**: S109-S14.
5. Gatzioufas Z, Seitz B. Determination of corneal biomechanical properties in vivo: a review. *Mater Sci Technol* 2015; **31**: 188-96.

6. Wollensak G, Spoerl E, Seiler T. Stress-strain measurements of human and porcine corneas after riboflavin–ultraviolet-A-induced cross-linking. *J Cataract Refract Surg* 2003; **29**: 1780-5.

7. Hjortdal JØ. Regional elastic performance of the human cornea. *J Biomech* 1996; **29**: 931-42.

8. Kling S, Remon L, Perez-Escudero A, Merayo-Lloves J, Marcos S. Corneal biomechanical changes after collagen cross-linking from porcine eye inflation experiments. *Invest Ophthalmol Vis Sci* 2010; **51**: 3961-8.

9. Yu JG, Bao FJ, Feng YF, Whitford C, Ye T, Huang YB, Wang QM, Elsheikh A. Assessment of corneal biomechanical behavior under posterior and anterior pressure. *J Refract Surg* 2013; **29**: 64-70.

10. Elsheikh A, Wang DF, Brown M, Rama P, Campanelli M, Pye D. Assessment of corneal biomechanical properties and their variation with age. *Curr Eye Res* 2007; **32**: 11-9.

11. Elsheikh A, Geraghty B, Rama P, Campanelli M, Meek KM. Characterization of age-related variation in corneal biomechanical properties. *J R Soc Interface* 2010; **7**: 1475-85.

12. Kling S, Marcos S. Effect of hydration state and storage media on corneal biomechanical response from in vitro inflation tests. *J Refract Surg* 2013; **29**: 490-7.

13. Rosales P, Marcos S. Pentacam Scheimpflug quantative imaging of the crystalline lens and intraocular lens. *J Refract Surg* 2008; **25**: 421-8.

14. Pérez-Escudero A, Dorronsoro C, Sawides L, Remón L, Merayo-Lloves J, Marcos S. Minor influence of myopic laser in situ keratomileusis on the posterior corneal surface. *Invest Ophthalmol Vis Sci* 2009; **50**: 4146-54.

15. Li T, Tian L, Wang L, Hon Y, Lam AK, Huang Y, Wang Y, Zheng Y. Correction on the distortion of Scheimpflug imaging for dynamic central corneal thickness. *J Biomed Opt* 2015; **20**: 56006.

16. Huang D, Li Y, Radhakrishnan S. Optical coherence tomography of the anterior segment of the eye. *Ophthalmol Clin North Am* 2004; **17**: 1-6.

17. Grulkowski I, Gora M, Szkulmowski M, Gorczynska I, Szlag D, Marcos S, Kowalczyk A, Wojtkowski M. Anterior segment imaging with Spectral OCT system using a high-speed CMOS camera. *Opt Express* 2009; **17**: 4842-58.

18. Ramos JLB, Li Y, Huang D. Clinical and research applications of anterior segment optical coherence tomography - a review. *Clin Exp Ophthalmol* 2009; **37**: 81-9.

19. Huang YP, Zheng YP, Wang SZ, Chen ZP, Huang QH, He YH. An optical coherence tomography (OCT)-based air jet indentation system for measuring the mechanical properties of soft tissues. *Meas Sci Technol* 2009; **20**: 015805.

20. Huang YP, Wang SZ, Saarakkala S, Zheng YP. Quantification of stiffness change in degenerated articular cartilage using optical coherence tomography-based air-jet indentation. *Connect Tissue Res* 2011; **52**: 433-43.

21. Chao CY, Ng GY, Cheung KK, Zheng YP, Wang LK, Cheing GL. In vivo and ex vivo approaches to studying the biomechanical properties of healing wounds in rat skin. *J Biomech Eng* 2013; **135**: 101009-8.

22. Dorronsoro C, Pascual D, Pérez-Merino P, Kling S, Marcos S. Dynamic OCT measurement of corneal deformation by an air puff in normal and cross-linked corneas. *Biomed Opt Express* 2012; **3**: 473-87.

23. Nguyen TM, Arnal B, Song SZ, Huang ZH, Wang RK, O'Donnell M. Shear wave elastography using amplitude-modulated acoustic radiation force and phase-sensitive optical coherence tomography. *J Biomed Opt* 2015; **20**: 016001.

24. Wang LK, Huang YP, Tian L, Kee CS, Zheng YP. Measurement of corneal tangent modulus using ultrasound indentation. *Ultrasonics* 2016; **71**: 20-8.

25. Hall TJ, Bilgen M, Insana MF, Krouskop TA. Phantom materials for elastography. *IEEE Trans Ultrason Ferroelectr Freq Control* 1997; **44**: 1355-65.

26. Kovesi P. Symmetry and asymmetry from local phase. *Tenth Australian Joint Conference on Artificial Intelligence* 1997: 185-90.

27. Anderson K, El-Sheikh A, Newson T. Application of structural analysis to the mechanical behaviour of the cornea. *J R Soc Interface* 2004; **1**: 3-15.

28. Boschetti F, Triacca V, Spinelli L, Pandolfi A. Mechanical characterization of porcine corneas. *J Biomech Eng* 2012; **134**: 031003.

29. Elsheikh A, Wang DF, Pye D. Determination of the modulus of elasticity of the human cornea. *J Refract Surg* 2007; **23**: 808-18.

30. Lu MH, Zheng YP, Huang QH. A novel method to obtain modulus image of soft tissues using ultrasound water jet indentation: a phantom study. *IEEE Trans Biomed Eng* 2007; **54**: 114-21.

31. Boyce BL, Grazier JM, Jones RE, Nguyen TD. Full-field deformation of bovine cornea under constrained inflation conditions. *Biomaterials* 2008; **29**: 3896-904.

32. Swartz T, Marten L, Wang M. Measuring the cornea: the latest developments in corneal topography. *Curr Opin Ophthalmol* 2007; **18**: 325-33.

Figure Legends:

Figure 1. Schematic of the inflation experiment proposed in this study which incorporates optical coherence tomography for the imaging of corneal responses. The system mainly consists of the parts of personal computer, OCT imaging, artificial anterior chamber where corneal sample is installed, pressure sensor and the IOP control subsystem.

Figure 2. (a) A schematic showing the designed geometry of the silicone corneal phantom and (b) a real sample of the phantom and a silicone strip with the same stiffness as the phantom.

Figure 3. Typical signal processing steps of the OCT images for the extraction of boundary of the anterior surface: (a) original image, (b) contrast-enhanced and speckle denoised image, (c) edge enhanced image, and (d) corneal OCT image with identified anterior surface boundary. Scale bars in (a) indicate a length of 1 mm.

Figure 4. (a) Typical change of the positions of the corneal anterior surface with test time during an inflation test and (b) typical displacement of cornea anterior surface at different locations. The displacement at a specific point - corneal apex is also shown in dash line. Three cycles of inflation and deflation are included in this test. Y indicates the lateral distance along an OCT image.

Figure 5. A thin shell model of cornea and critical factors in inflation test. T: corneal thickness, p: intraocular pressure, R: curvature of the corneal surface.

Figure 6. Typical IOP-apex displacement curves of (a) a corneal phantom and (b) a porcine cornea tested in this study.

Figure 7. Comparison of the corneal Young's modulus obtained by the inflation test and the tensile test.

Figure 8. Typical results for the mapping of a corneal phantom surface displacement with IOP change from 10 mmHg to 90 mmHg. (a) A 3D map of the corneal anterior surface at IOP_1 = 10 mmHg; (b) A 3D map of corneal anterior surface at IOP_2 = 90 mmHg; (c) Mapping of corneal surface displacement from IOP_1 to IOP_2; (d) Corneal surface displacement at various distances away from corneal center as indicated by those lines in (c). L is the radius of the circle shown in (c).

Figure 9. Typical results for the mapping of a porcine corneal surface displacement with IOP change from 10 mmHg to 90 mmHg. (a) A 3D map of the corneal anterior surface at IOP_1 = 10 mmHg; (b) A 3D map of corneal anterior surface at IOP_2 = 90 mmHg; (c) Mapping of corneal surface displacement from IOP_1 to IOP_2; (d) Corneal surface displacement at various distances away from corneal center as indicated by those lines in (c). L is the radius of the circle shown in (c).

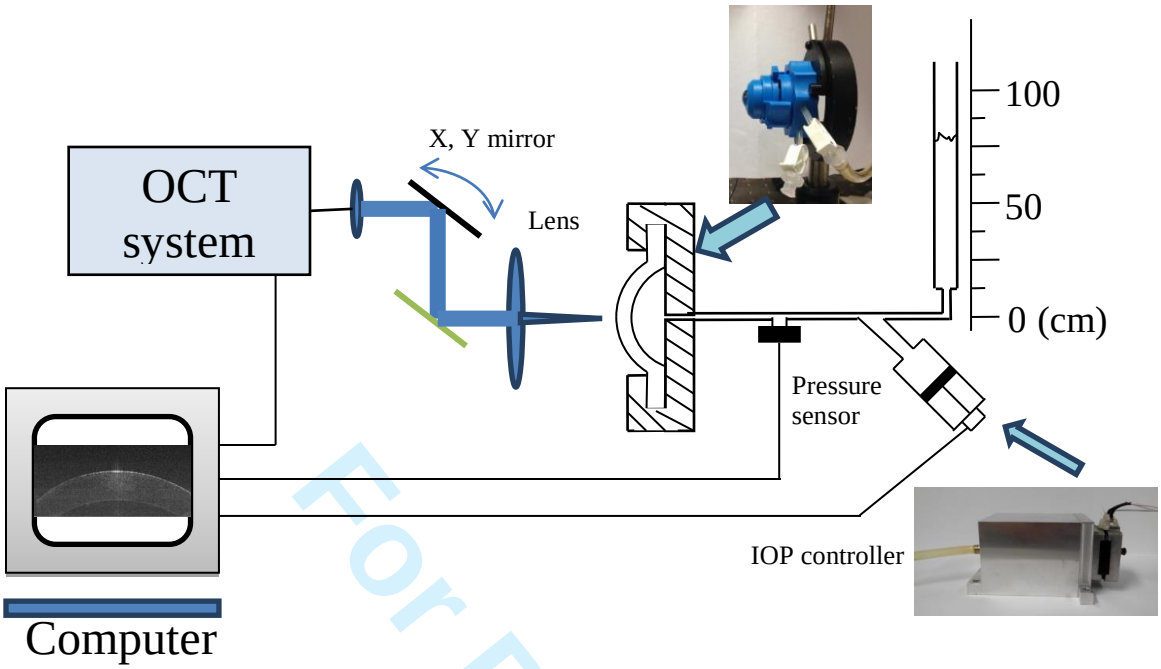

Figure 1

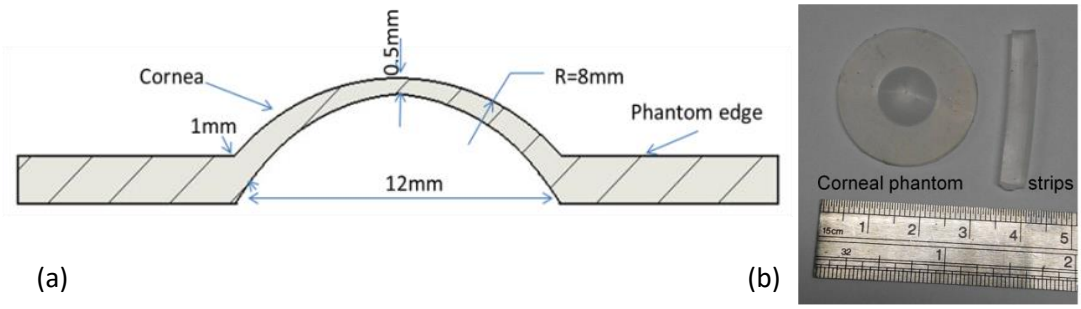

Figure 2

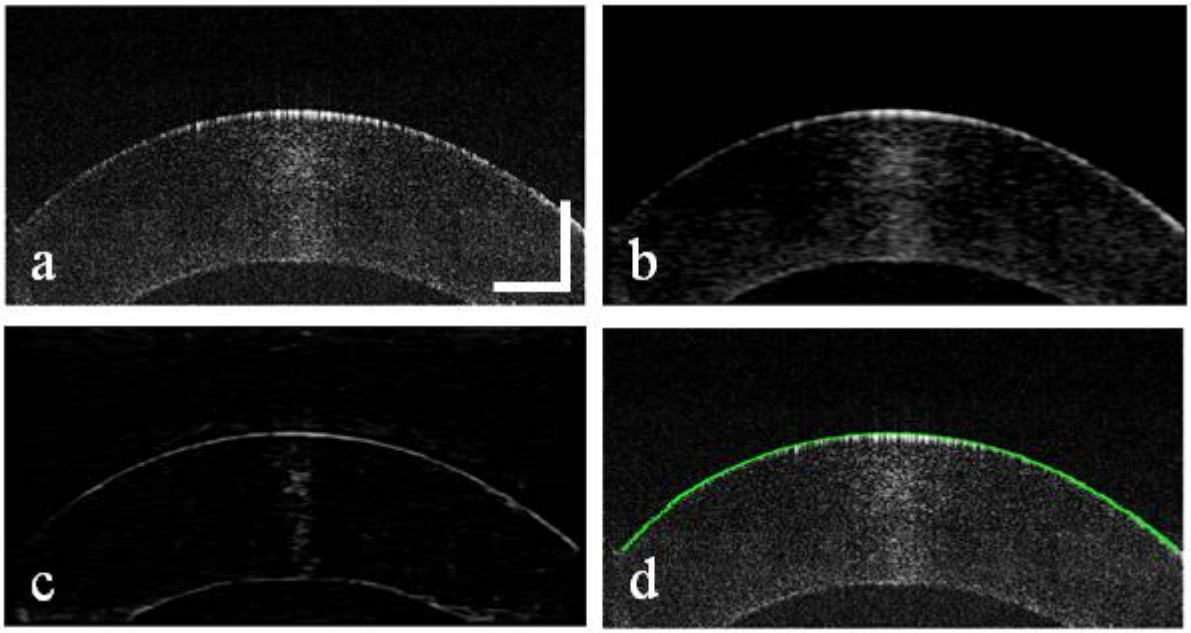

Figure 3

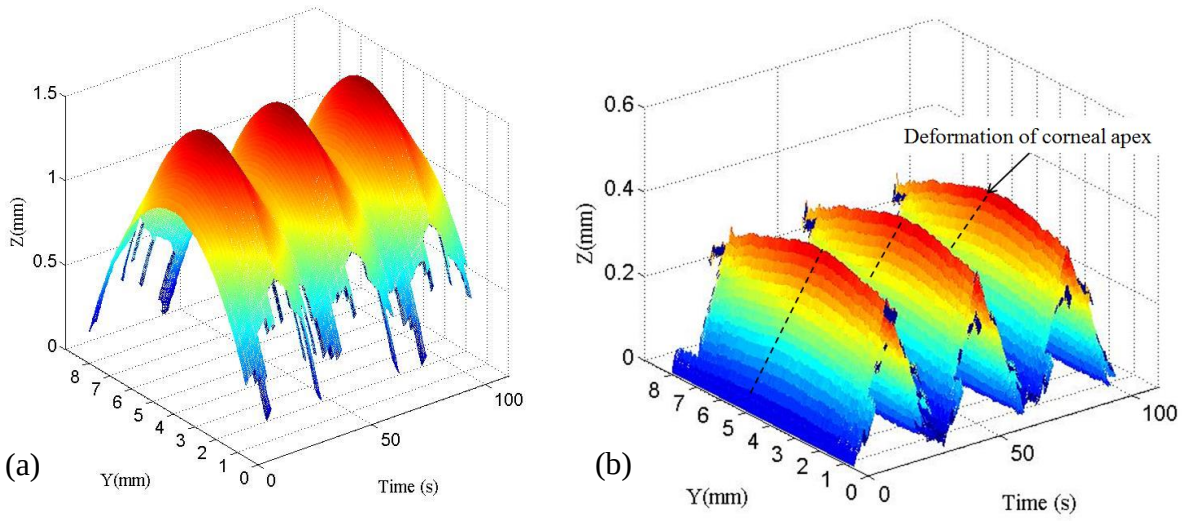

Figure 4

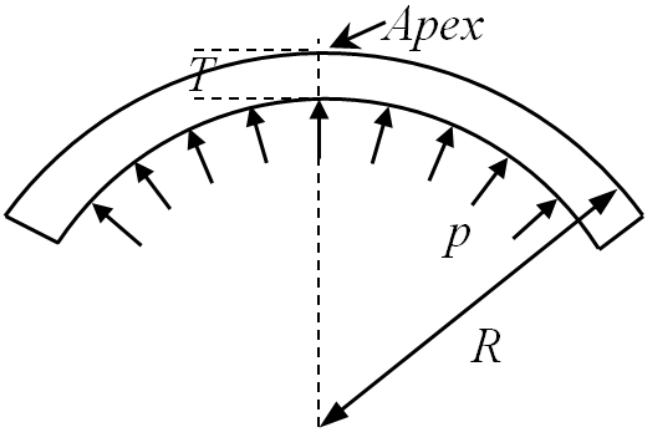

Figure 5

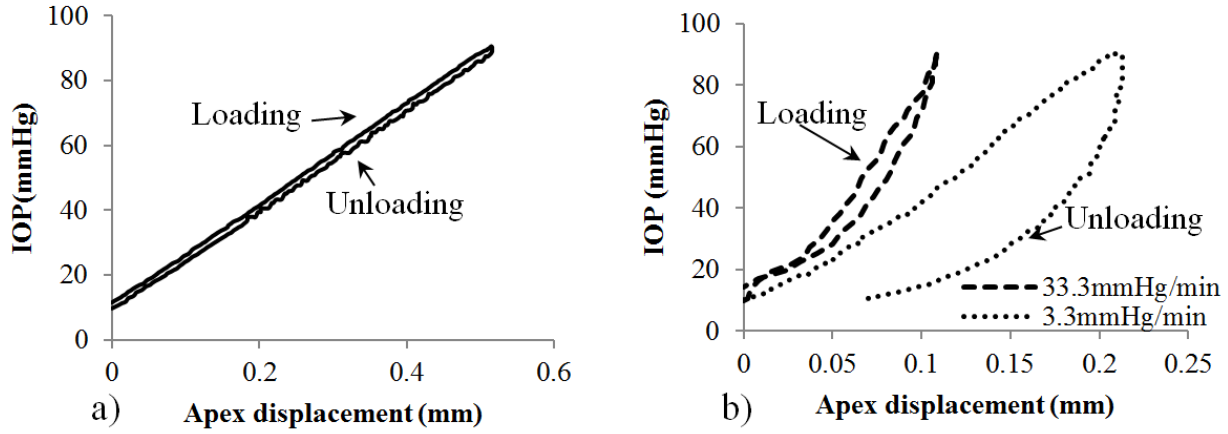

Figure 6

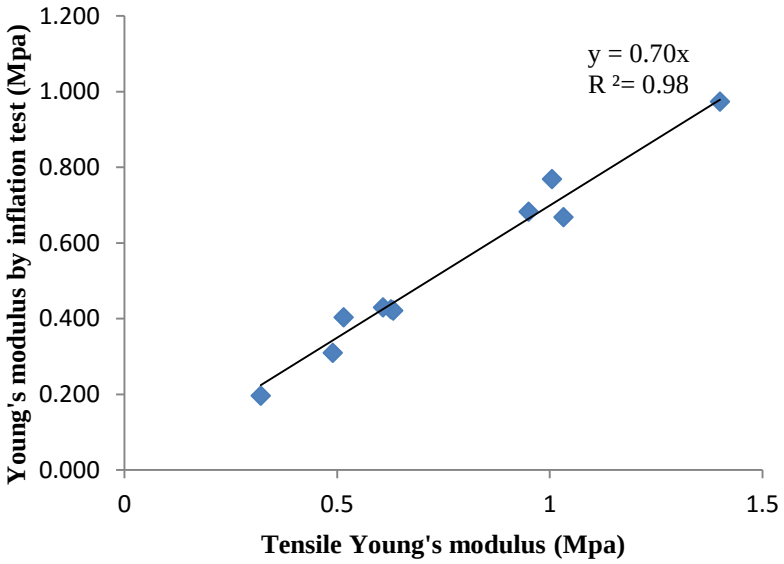

Figure 7

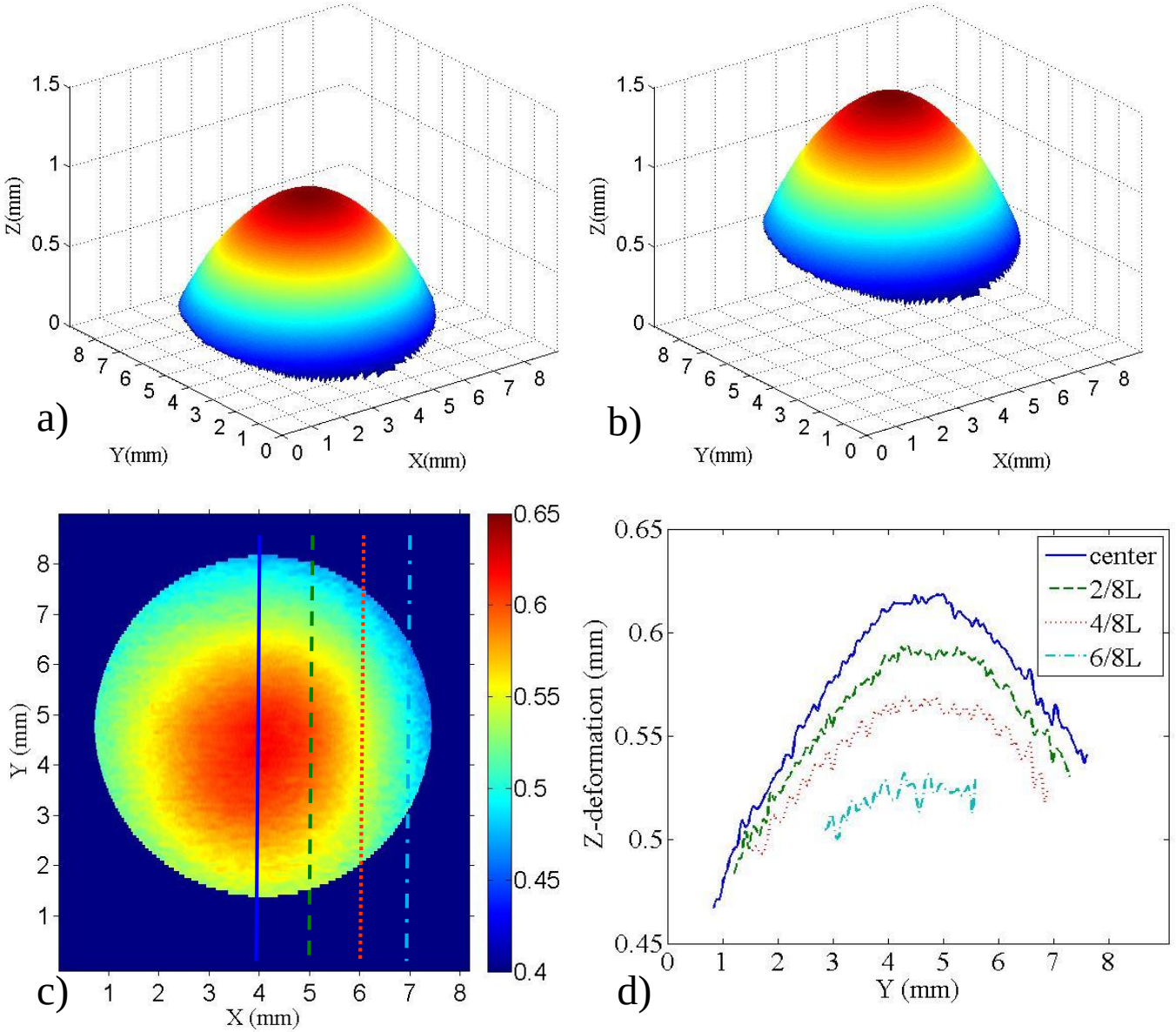
a)
Z(mm)
Y(mm)
X(mm)
b)
Z(mm)
Y(mm)
X(mm)
c)
Y (mm)
X (mm)
d)
Z-deformation (mm)
Y (mm)
center
2/8L
4/8L
6/8L

Figure 8

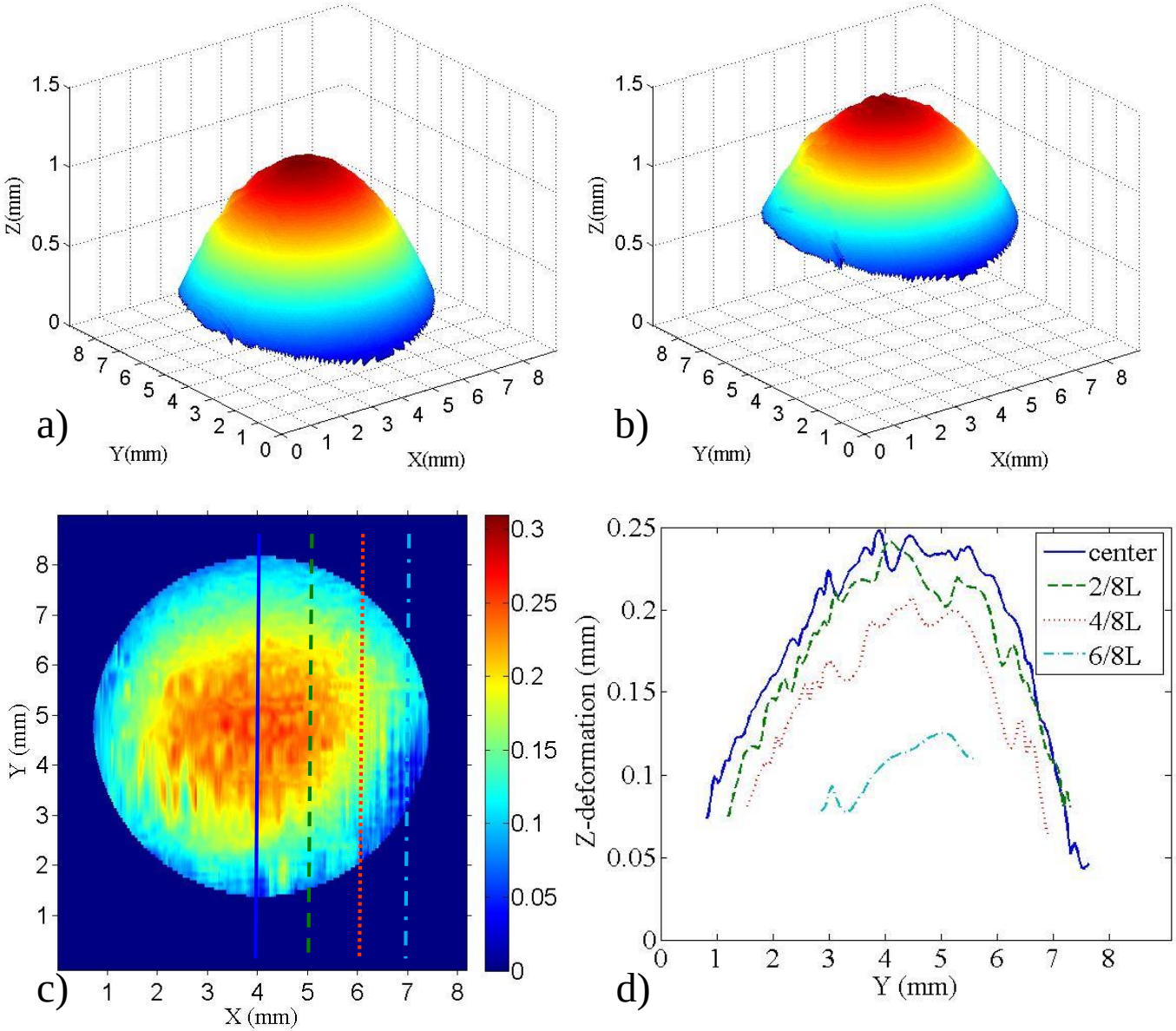
a)
Z(mm)
Y(mm)
X(mm)
b)
Z(mm)
Y(mm)
X(mm)
c)
Y (mm)
X (mm)
d)
Z-deformation (mm)
Y (mm)
center
2/8L
4/8L
6/8L

Figure 9